

Sustainable Aviation Fuel Molecules from (Hemi)Cellulose: Computational Insights into Synthesis Routes, Fuel Properties, and Process Chemistry Metrics

Chin-Fei Chang,^{II} Kristin Paragian,^{II} Sunitha Sadula, Srinivas Rangarajan,* and Dionisios G. Vlachos*



Cite This: *ACS Sustainable Chem. Eng.* 2024, 12, 12927–12937



Read Online

ACCESS |

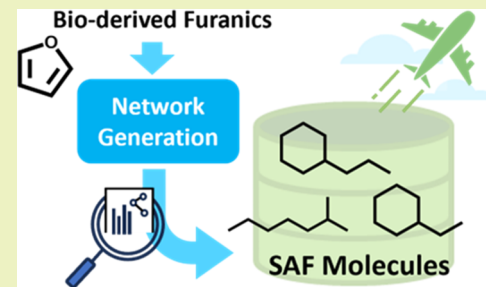
Metrics & More

Article Recommendations

Supporting Information

ABSTRACT: Production of sustainable aviation fuels (SAFs) can significantly reduce the aviation industry's carbon footprint. Current pathways that produce SAFs in significant volumes from ethanol and fatty acids can be costly, have a relatively high carbon intensity (CI), and impose sustainability challenges. There is a need for a diversified approach to reduce costs and utilize more sustainable feedstocks effectively. Here, we map out catalytic synthesis routes to convert furanics derived from the (hemi)cellulosic biomass to alkanes and cycloalkanes using automated network generation with RING and semiempirical thermochemistry calculations. We find >100 energy-dense C₈–C₁₆ alkane and cycloalkane SAF candidates over 300 synthesis routes; the top three are 2-methyl heptane, ethyl cyclohexane, and propyl cyclohexane, although these are relatively short. The shortest, least endothermic process chemistry involves C–C coupling, oxygen removal, and hydrogen addition, with dehydracyclization of the heterocyclic oxygens in the furan ring being the most endothermic step. The global warming potential due to hydrogen use and byproduct CO₂ is typically 0.7–1 kg CO₂/kg SAF product; the least CO₂ emitting routes entail making larger molecules with fewer ketonization, hydrogenation, and hydrodeoxygenation steps. The large number of SAF candidates highlights the rich potential of furanics as a source of SAF molecules. However, the structural dissimilarity between reactants and target products precludes pathways with fewer than six synthetic steps, thus necessitating intensified processes, integrating multiple reaction steps in multifunctional catalytic reactors.

KEYWORDS: jet fuels, GWP, biomass, synthesis routes, furans, fuels



INTRODUCTION

Commercial aviation accounts for 11% of transportation greenhouse gas (GHG) emissions.^{1,2} At the projected growth rate of the aviation industry, the emissions can reach 1.9 GtCO₂ in 2050, ~2.6 times the 2021 values.³ Achieving net-zero carbon emissions by 2050 will require the development of sustainable aviation fuels (SAFs), drop-in liquid hydrocarbon fuels created from waste, renewable materials, and gaseous carbon sources. According to the US 2021 Aviation Climate Action Plan, SAF offers a critical near-term solution to reduce greenhouse gas emissions.¹ To meet the US climate goals and aviation demand, 3 billion gallons by 2030 and 35 billion gallons by 2050 should be produced.⁴ According to the recent Department of Energy (DOE) billion tons report, the amount of available biomass is adequate for SAF production.⁵

Aviation fuels contain hydrocarbons comprising a range of molecular sizes and structures. For instance, Jet A, a conventional jet fuel used as a benchmark for SAF's molecular composition and fuel properties, contains C7–C18 hydrocarbons, including *n*-alkanes, iso-alkanes, cycloalkanes, and aromatics (see Figure 1 for the relative composition, adapted from the DOE report⁶ with original data from ref 7). As of 2023, 11 conversion processes for SAF production⁸ have been

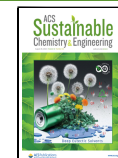
approved for commercial flights, but these lack aromatics and cycloalkanes that can impart desirable properties.^{9–11,12,13} Due to the lack of all components, blending SAF with petroleum fuel is inevitable but undesirable. Recent biobased cycloalkane efforts utilizing lipid feedstocks, cellulosic, and lignin address this challenge, but none have reached commercialization.^{1,14–29} These methods include condensation of furanic aldehydes and cyclic ketones,^{30–38} alkylation of furfural-derived cycloalkanes with phenolics,^{39–41} conversion of lignin-derived phenols,^{42–45} Robinson annulation of furfural and 2,4-pentanedione,^{46–48} and conversion of cyclic ketones to polycyclic alkanes.^{49–53} Hydroxyalkylation/alkylation of furans and condensation^{54–57} have been reported to convert biomass-derived small molecules, including furfural, furfuryl alcohol, 5-hydroxymethylfurfural, cyclic ketones, phenolics, acyclic

Received: May 21, 2024

Revised: August 2, 2024

Accepted: August 6, 2024

Published: August 13, 2024



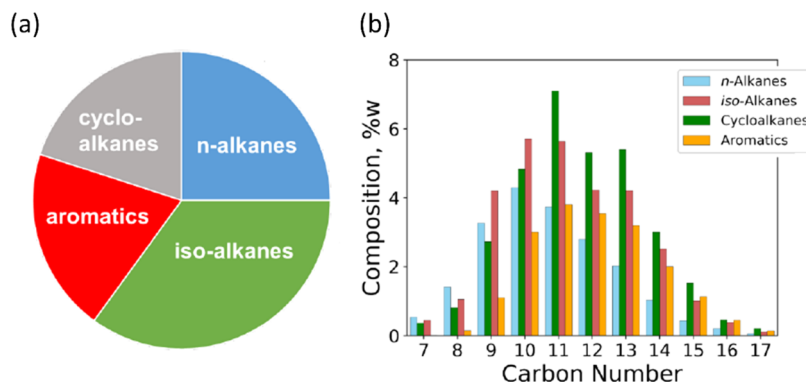


Figure 1. Composition of average jet fuel A. (a) Fractions and (b) distribution of different components. Adapted from DOE report.⁶

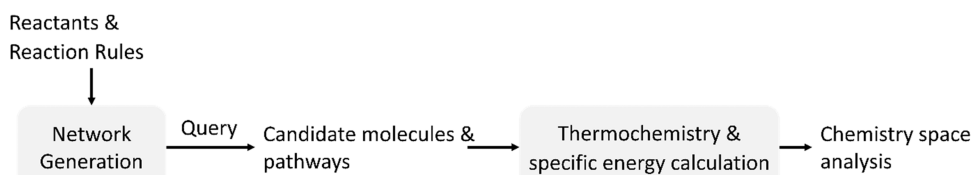


Figure 2. Computational workflow for exploring synthesizable molecules and the chemistry space for sustainable aviation fuels (SAFs).

ketones, cyclic alcohols, furans, esters, and alkenes to high-density cycloalkanes.¹⁵ Despite significant progress, challenges remain in developing more efficient catalytic routes for producing cycloalkanes with less hydrogen, lower temperatures and pressures, greater selectivity, and lower carbon footprints. Even with current and emerging technologies, achieving the targeted SAF volumes is impossible. Thus, new conversion technologies capable of generating all of the SAF components from abundant, renewable feedstocks are essential for 100% drop-in SAF.¹²

Furans, including furfural and 5-hydroxymethylfurfural (HMF), derived from abundant lignocellulosic sugars, can be converted to aromatics in high yield.⁵⁸ For example, HMF can be transformed into dimethylfuran (DMF) and then *para*-xylene via Diels–Alder cycloaddition-dehydration with ethylene, with >90% yield^{59–63} to synthesize SAF. Such routes have, however, not been explored much, and delineating the best candidate SAF molecules and synthesis routes can guide the development of novel processes. However, since furanics are oxygenated rings with 4–6 carbon atoms, SAF synthesis would require C–C bond formation to increase the carbon chain, oxygen removal, and hydrogenation of C–C unsaturated bonds, likely with unintuitive combinations;^{64–68} there exist many possible options. Manual curation and analysis of these options are time-consuming and cumbersome; instead, here, we use automated reaction network generation based on expert knowledge of catalytic chemistries^{63,66,69–73} to chart the synthesis space for upgrading furans to linear, branched, and cycloalkanes. We identify synthesizable SAF candidates with high energy density and synthetic routes of low global warming potential (GWP), low energy use, and minimum number of reaction steps.

METHODS

The computational workflow, shown in Figure 2, comprises four steps: (1) Generation of a reaction network of plausible reactions, demarcating the synthesis space. We use the Rule Input Network Generator (RING)^{74,75} with a set of initial biomass-derived reactants and heterogeneous catalysis reaction rules; (2) Postgeneration queries

in RING to discover suitable SAF molecules and their synthetic pathways; (3) Estimation of the thermochemistry of molecules and pathways and molecule-specific energy; and (4) Analysis of the ensuing chemistry space to elicit specific pathway- and overall network-level insights. RING is employed as the network generator, in view of its flexibility in describing rules and searching for pathways.

Six (6) biomass-derived reactants (*viz.*, furan, 2-methyl furan, 2,5-dimethylfuran, furfural, HMF, and acetic acid) and molecular H₂ along with 11 reaction classes (encoded in 22 rules) were provided to RING. These methyl furans can be derived from furfural (hemicellulose) and HMF (cellulose) in a single step.^{76–78} Acetic acid is a common byproduct. The reaction classes were selected to grow the carbon chain to the SAF range, remove the oxygen atoms to improve the energy density and thermal stability, and saturate bonds to improve the oxygen stability and energy density. They include acylation, aldol condensation, dehydro-decyclization, Diels–Alder, hydrodeoxygenation (HDO), hydroxylalkylation/alkylation, ketonization, hydrogenation, alcohol dehydration to alkenes or ethers, alkylation, and (de)hydrogenation. The reaction classes and associated RING rule(s) are detailed in Table S1 in Supporting Information Section S1.

Global constraints prevent highly reactive or unphysical molecules, such as those including (1) three consecutive C=C=C or ketene fragments (O=C=C), (2) acyclic molecules with more than two C=C, and (3) cyclic molecules with rings containing fewer than four C atoms. Also, we restrict the maximum molecular size to 22 carbon atoms in the jet fuel range. Other specific constraints are presented in Table S1. The heat of formation of molecules and the heat of reactions were computed using pGrAdd, a Python group additivity package.^{79,80} The specific energy (MJ/kg) of molecules was calculated using the heat of formation (along with heat of formation of combustion products, water and carbon dioxide both in the gas phase, taken from NIST).

RESULTS AND DISCUSSION

The generated reaction network includes 223,107 species among 363,840 reactions, underlying the chemistry richness and the need for an automated tool. The molecules include alkanes, olefins, aromatics, alcohols, acids, ketones, and aldehydes (see Figure S3 of Section S4). Due to the absence of oxygen in jet fuels, we focus hereafter only on hydrocarbons, and specifically nonaromatic ones (although aromatics are also

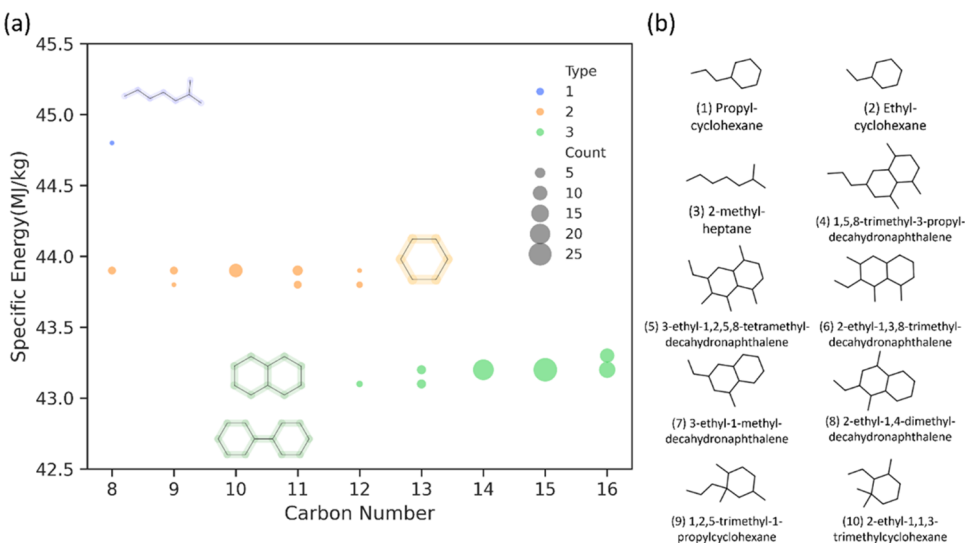


Figure 3. (a) Specific energy of 109 molecules vs carbon number. Three types of molecular structures are colored blue (acyclic alkanes), orange (monocycloalkanes), and green (dicycloalkanes), with an example molecule for each. The circle size is proportional to the number of molecules with the same carbon number and nearly equal specific energy. (b) A subset of the 109 SAF candidates.

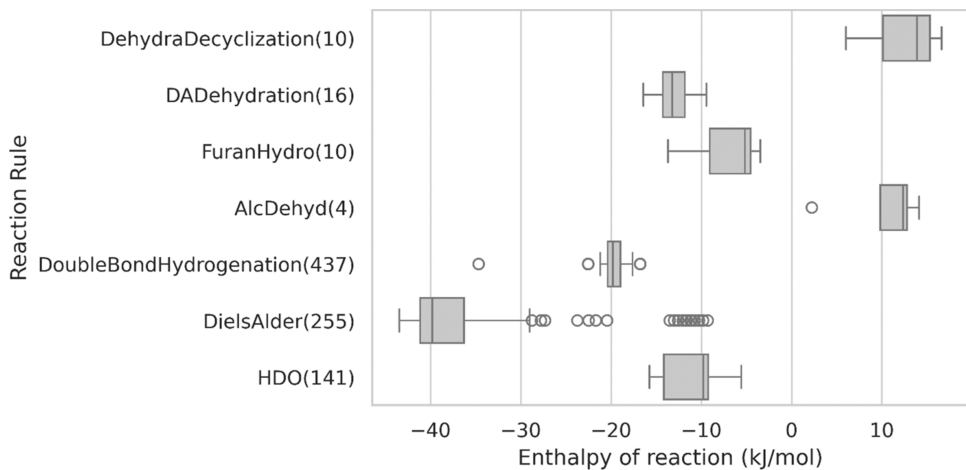


Figure 4. Distribution of the enthalpy of the reaction for different reaction rules. The number of data points for each rule is given in parentheses. The upper/lower boundary of the whisker represents the maximum/minimum value in the data set (outliers excluded). The gray box covers the observed data ranges from the first quartile to the third quartile with the median presented (line within the box). Outliers are presented in hollow dots.

needed for SAFs). Of all species, 109 molecules are nonaromatic, saturated hydrocarbons with 8–16 carbon atoms (C_8 – C_{16}) in the jet-fuel range; only one was found to be acyclic (2-methyl heptane), with the rest having at least one six-membered ring (see Figure 3b for a partial list, the whole list is in Figure S1 of Section S2 and a supporting interactive tool to visualize molecules and pathways is provided in Section S5). Interestingly, the absence of C_8 – C_{16} isoparaffins indicates that other reactants are required to make such molecules in a few steps.

The specific energy of these candidates (Figure 3a) is weakly dependent on the carbon number and only moderately dependent on the structure. Acyclic alkanes exhibit higher specific energy (>44 MJ/kg) than other hydrocarbons, while monocycloalkanes fall within the 43.5 MJ/kg range and dicycloalkanes around 43 MJ/kg. These could be SAF candidates based on (1) having high specific energy (>43 MJ/kg), according to the DOE's specifications,⁶ and (2) being liquids under typical operating conditions. The three highest

specific energy candidates are 2-methyl heptane (44.82), propyl cyclohexane (43.89), and ethyl cyclohexane (43.88); however, given their size (8–9 carbon atoms), they are expected to contribute only up to 2 wt % of a typical jet fuel mixture (Jet A).

We queried RING to identify short reaction pathways to each molecule (specifically, by setting the maximum path length up to two more steps than the shortest possible path), as this is a simple metric of economics; fewer steps lead to lower capital cost because, often, each step is a separate reactor (or a reaction zone in a multifunctional reactor). When pathways contain bimolecular steps (two reactants), the synthesis steps to both reactants were traced to correctly compute associated metrics (discussed later). This query yielded 315 unique pathways, indicating a rich SAF product slate and synthesis options. Figure S4 of Section S4 (Supporting Information) shows the statistics of starting reactants for these pathways; furan (picked 195 times), 2-methyl furan (345), and furfural (172) are the prominent

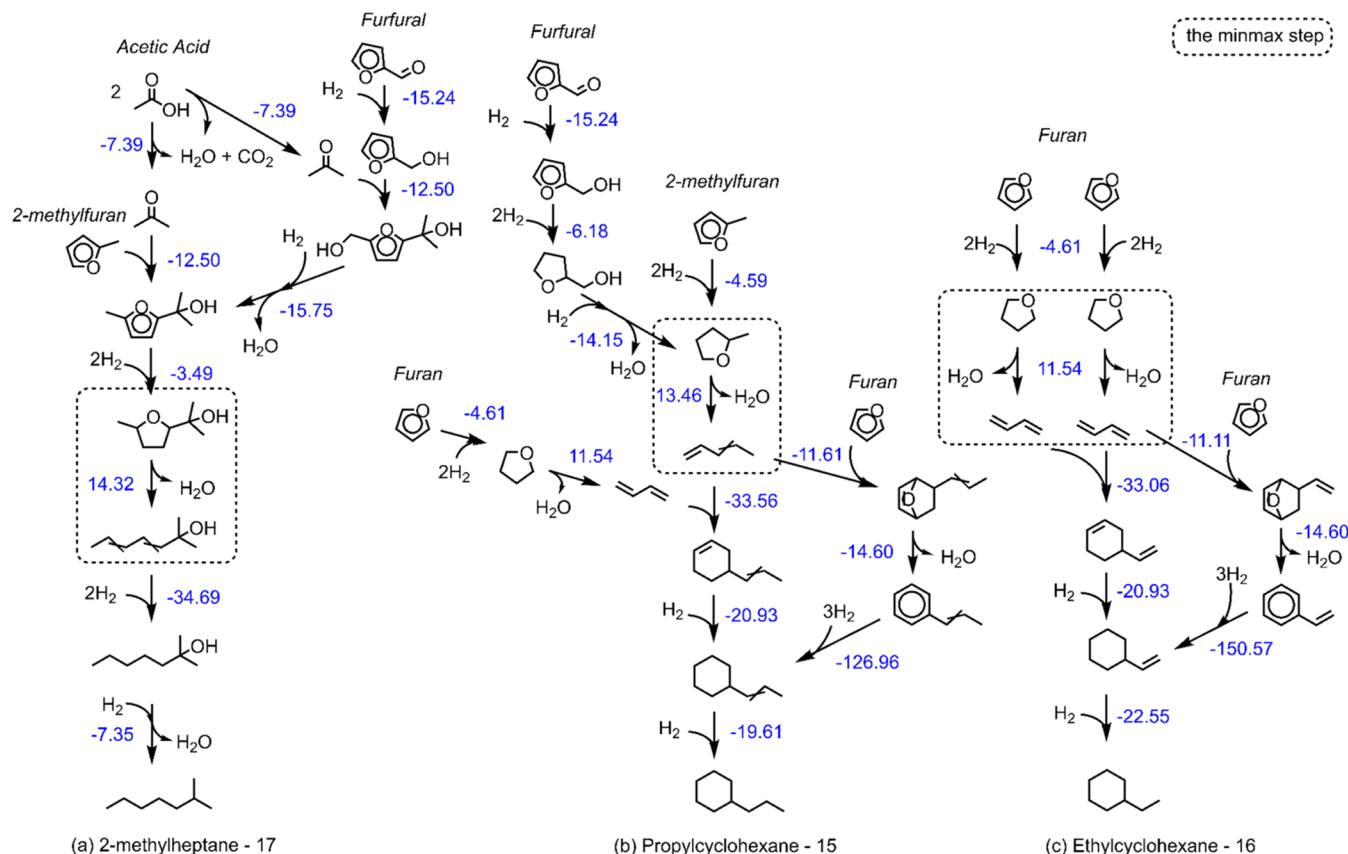


Figure 5. Synthesis routes (“min–max”) to the highest specific energy molecules (names and their index in RING given at the bottom). Each step is annotated by its reaction enthalpy at 298 K (kJ/mol), shown in blue. The most endothermic step in each case is enclosed in a dashed box.

starting reactants and may participate more than once in some pathways. Interestingly, HMF was never picked as a reactant, indicating that the number and type of functional side groups determine whether it is invoked, given that we seek only short pathways (note that 2,5-dimethylfuran is produced from HMF in one step via HDO). Figure S5 shows a histogram of the reaction distribution categorized by rules. Hydrogenation (occurring 1446 times), HDO (389), Diels–Alder (577), and dehydra-decyclization (839) are featured prominently. In contrast, alkylation, a well-known C–C bond-forming reaction, is not present in these pathways, as it does not form saturated hydrocarbons in the given number of steps or makes molecules containing at least one oxygen atom. Correlation analysis of the 315 queried pathways using a novel fingerprint (Section S3.1) provided network-level insights into several reactant–rule and rule–rule relationships. While detailed insights are provided in Section S3.2, we note here that some unintuitive relationships were identified from Figure S2, for example, furan hydrogenation, Diels–Alder, and dehydra-decyclization are correlated, indicating that these steps often occur together to saturate furans, remove oxygen, and form C₆ rings.

Given this rich space of SAF candidates and synthesis routes, the questions “What SAF molecule(s) to make?” and “How to make it (them)?” need to be addressed simultaneously. This requires a wholistic analysis of the entire reaction network. Here, instead, we analyze our reduced search space of 109 molecules and 315 pathways by employing screening metrics, specifically two independent contributors to the total GWP: (1) reaction endothermicity, related to process heat, and (2)

CO₂ release from the process chemistry, arising from the stoichiometry and coreagent (H₂) use.

The reaction enthalpy and, thus, the endothermicity depend on the reaction rule and the structure and functionalities of the reactants and products. Figure 4 presents the reaction enthalpy of the reaction rules that occur at least four times in all queried pathways (see Figure S5 of Section S4 for the frequency distribution of each rule). HDO, Diels–Alder, dehydration in Diels–Alder (termed DADehydration), double bond hydrogenation, furan hydrogenation (termed FuranHydro), alcohol dehydration (AlcDehyd), and dehydra-decyclization are moderately endothermic or exothermic (enthalpy varies between –40 to 20 kJ/mol). The most endothermic reactions are dehydra-decyclization and alcohol dehydration, while Diels–Alder and benzene ring hydrogenation are significantly more exothermic (reaction enthalpy ranging from –50 to –150 kJ/mol; note that highly exothermic steps are not included in Figure 4). The variability across the reaction rules and even within a rule implies that all pathways must be enumerated and evaluated step-by-step to identify bottlenecks. In particular, the step with the highest endothermicity in a pathway can be a surrogate metric for both energy requirement (and associated CO₂ emissions) and thermodynamic bottlenecks; therefore, we seek the pathway with the smallest enthalpy of the highest endothermicity step (the “min–max” path) for this metric. Figure 5 shows the min–max pathways to the three most energy-dense molecules. As seen in Figure 5, (1) ketonization, hydroxyalkylation, hydrogenation, dehydra-decyclization, and hydrogenolysis produce 2-methyl heptane (Figure 5a), and (2) hydrogenation, dehydra-decyclization,

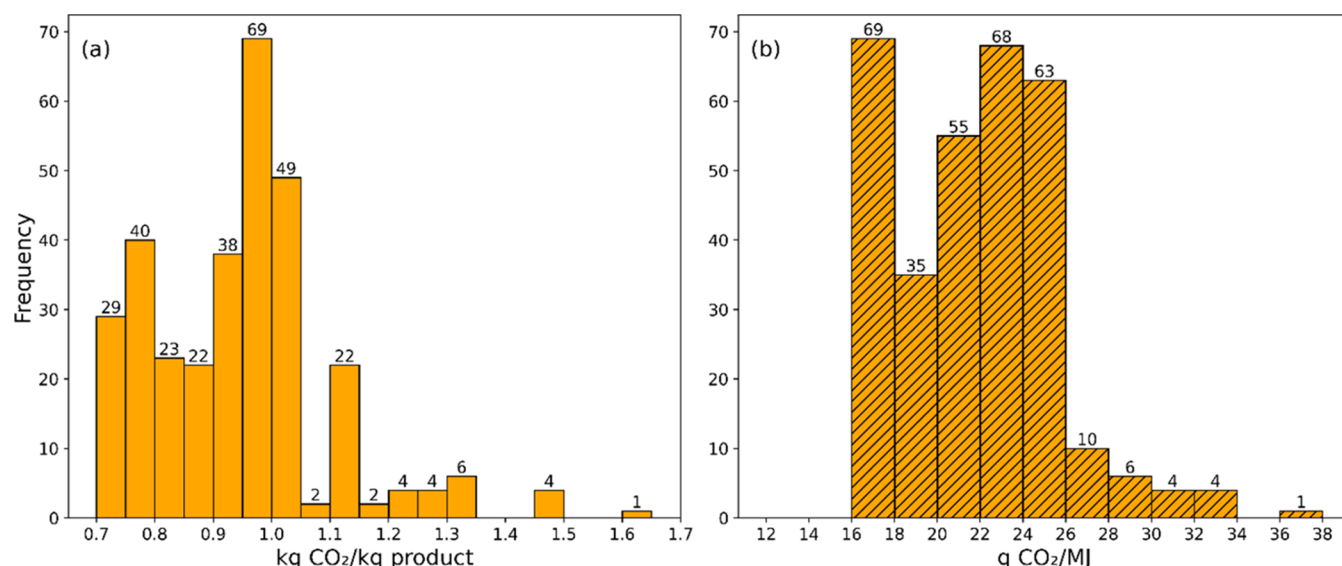


Figure 6. Histogram of (a) $\text{CO}_{2\text{eq}}$ (kg-CO₂/kg product) and (b) carbon intensity (g-CO₂/MJ) from process chemistry, considering emissions from the hydrogen use and the CO₂ byproduct of each pathway.

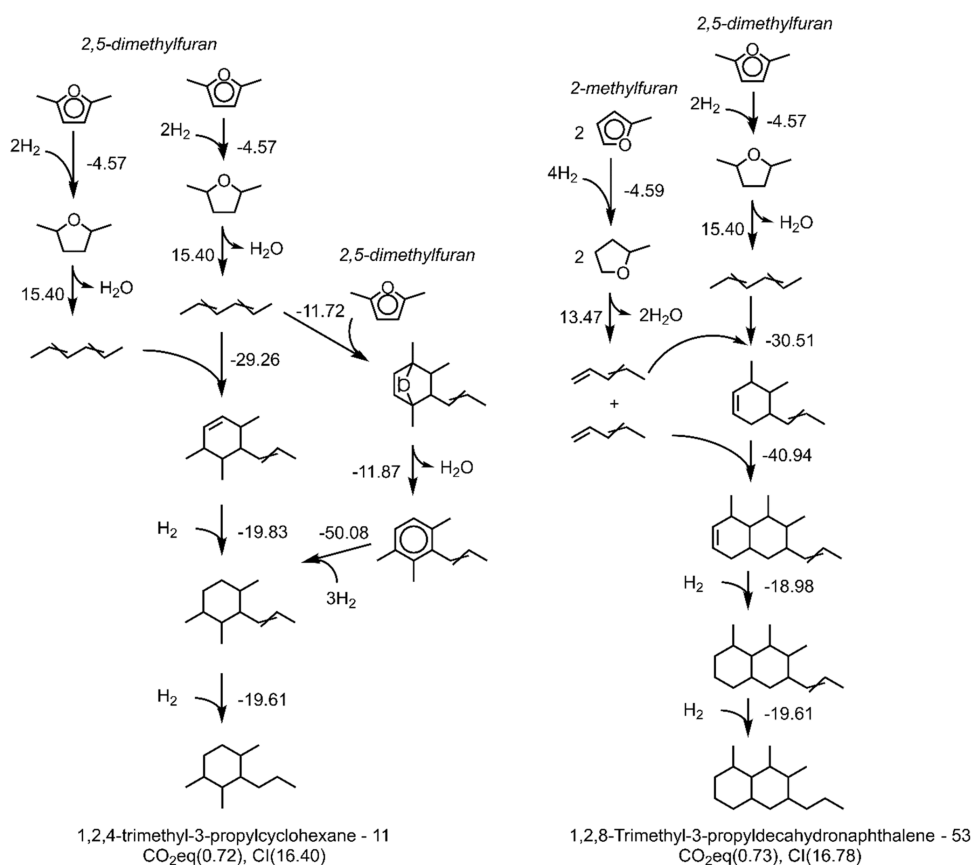


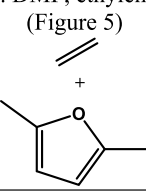
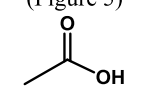
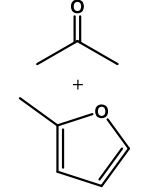
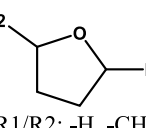
Figure 7. Routes to the lowest two CO_2 -producing synthesis routes. Names, network indices (for easy reference in Sections S2 and S3), and their $\text{CO}_{2\text{eq}}$ (in kg-CO₂/kg-product), and carbon intensity (CI) index (in g-CO₂/MJ) are shown at the bottom.

Diels–Alder with subsequent dehydration, and hydrogenation result in propyl and ethyl cyclohexane (Figure 5b,c), respectively. Pathways to all three candidates involve dehydro-decyclization as the most important endothermic step, consistent with Figure 4.

Alternative energy-based metrics include the sum of (i) all endothermic reaction enthalpies (termed “Endosum”) for the

required process heat and (ii) the absolute values of all reaction enthalpies (“AbsdHsum”) as a descriptor of the operational cost (based on empirical relations identified for chemical and energy industries).⁸¹ At this stage, since we do not consider detailed process design, we assume no heat integration as an extreme limit. Figures S6 and S7 of Section S4 show the pathways to the three energy-dense candidates

Table 1. Experimental Evidence of Some of the Identified Reactions for SAF Synthesis and Their Selectivity Challenges^{86–103}

Reactants	Rule	Product	Catalyst and conditions	Yield, Y/ Selectivity, S (%)	Side reactions/ challenges
I. DMF, ethylene (Figure 5) 	Diels-Alder ^{86–90}	p-Xylene	Zeolites, aliphatic solvents, 300–600 °C	75% (S) with H-Y Zeolite	Hydrolysis of DMF to 2,5-hexanedione; alkylation of p-xylene; polymerization of 2,5-hexanedione.
II. Acetic acid (Figure 5) 	ketonization ^{71, 91}	acetone	Zeolites	100% (S) with HZSM-5	Sequential aldol condensation reactions of acetone
III. 2-MF, acetone (Figure 5) 	Hydroxy-alkylation/alkylation (HAA) ^{66, 67, 92–97}	C8 furan or C13 difuran adduct	Graphene oxide	90% (Y)	Typically results in difuran synthesis
IV. THF, 2-MTHF, 2,5-DMTHF (Figure 5/Figure 7)  R2 R1/R2: -H, -CH ₃	Dehydra-decyclization ^{98–103}	C4–C6 dienes	Zeolites	>70% (S) with P-SPP	THF ring opening without dehydration to 3-butene-1-ol, retro-Prins condensation to propylene and formaldehyde

with the lowest “Endosum” and “AbsdHsum” values; as expected, the AbsdHsum pathways have fewer instances of highly endothermic and exothermic steps (Diels–Alder, dehydra-decyclization). The “min-max”, “Endosum”, and “AbsdHsum” pathways to all other candidates can be identified using our interactive tool provided in the [Supporting Information](#).

Converting biomass oxygenates to saturated alkanes requires (i) removing oxygen via dehydration, dehydra-decyclization, decarboxylation through ketonization, and HDO, and (ii) adding hydrogen to saturate the C–C bonds. Therefore, aside from the process heat, the process chemistry too causes carbon emissions due to (1) H₂ use which contributes to CO₂ emissions (~10 kg-CO₂/kg-H₂, assuming production by steam methane reforming)⁸² and (2) byproduct CO₂ release, e.g., in ketonization. Both H₂ and the byproduct CO₂ are significantly involved in the synthesis routes. For instance, we found that more than 260 of the 315 pathways require ≥8 mol-H₂/mol-product ([Figure S8](#)), with 12 pathways requiring ≤5 mol-H₂/mol-product, indicating the generally high hydrogen requirements. In addition, 173 of the 315 pathways coproduce ≥4 mol-H₂O/mol-product ([Figure S8](#)), indicating that a significant fraction of hydrogen removes oxygen. Indeed, a correlation analysis ([Figure S9](#)) suggests that water generation significantly correlates with H₂ consumption. Further, 23 of the 315 pathways release CO₂ through ketonization ([Figure S8](#)), and CO₂ production is negatively correlated with the H₂

demand but positively correlated with coproduced water ([Figure S9](#)). Therefore, to assess the net CO₂ emissions from the process chemistry alone, i.e., byproduct CO₂ and coreagent H₂, we summed these two CO₂ sources, denoted as CO_{2eq} (measured in kg-CO₂/kg-product). [Figure S10](#) of Section S4 shows the pathways with the lowest CO_{2eq} to the three most energy-dense candidates. Interestingly, all routes are already shown in [Figure 5](#); the lowest CO_{2eq} for 2-methyl heptane, propyl- and methyl-cyclohexane is 1.27, 0.97, and 1.08 kg-CO₂/kg-product, respectively.

The distribution of CO_{2eq} across all 315 pathways ([Figure 6](#)) shows that more than two-thirds have a footprint of 0.7–1 kg-CO₂/kg-product (lower than the top-3 energy-dense molecules) due to their lower hydrogen demand. The candidate molecules with the lowest CO_{2eq} are shown in [Figure S11](#) of Section S4. The routes to the top two candidates are shown in [Figure 7](#), with the respective “min-max,” “EndoSum,” and “AbsdHsum” pathways given in [Figure S12](#). As shown in [Figure 7](#), these molecules tend to be larger (thereby having a higher product mass and hence a lower CO_{2eq}) while requiring the same amount of H₂ as the most energy-dense molecules shown in [Figure 5](#). The two molecules in [Figure 7](#) are novel candidates, never reported in the context of SAFs. We note that the C₁₂ product can contribute up to 5 wt % of a typical jet fuel such as jet A, representing one of the larger fractions, while the C₁₆ can be up to 1%. [Figure 6](#) also shows the carbon intensity (CI) of the fuel candidates measured as g-CO₂ per

MJ of energy; as can be seen, most of the candidates are in the range of 16–30 g-CO₂/MJ.

A vital sustainability metric is the theoretical atom efficiency, viz., the fraction of atoms of reactants retained in the products in a pathway (not considering selectivity limitations). We computed the theoretical carbon atom efficiency and found that 95 fuel candidates have at least one pathway with an ideal 100% carbon atom efficiency. In contrast, 14 molecules have a carbon atom efficiency of 85 to 91% (see Figure S13 of Section S4 for a list). The relatively high carbon atom efficiency is attributed to ketonization being the only reaction leading to carbon loss. Since ketonization is primarily used to synthesize acetone, allowing this molecule as an initial reactant avoids this reaction altogether. These are upper bound values that would decrease depending on the selectivity and number of steps in a pathway.

Many steps identified in Figures 5 and 7 have been experimentally demonstrated or have a close analogue to experimentally observed ones (Table 1). The selectivity challenges are well understood, thereby reinforcing the validity of this approach. Here, we discuss several of these cases. First, the pathway to 2-methyl heptane (Figure 5) requires an acid-catalyzed step of acetone and 2-methyl furan (or, furfuryl alcohol); the C₈ adduct can react with another furan to form a difuran leading to a larger (C₁₃) product⁸³ (Table 1, entry III). Although this product can eventually be hydro-deoxygenated to a SAF-compatible branched alkane, additional steps prevent it from being generated in the network. The selective synthesis of the C₈ product in Figure 5 will require tuning the acid strength of the catalyst and the ratio of the reactants to enable the first hydroxyalkylation step but avoid the second alkylation step. However, diminished selectivity in this step is not detrimental, since the eventual C₁₃ product is an SAF candidate molecule. Therefore, this represents an example where low selectivity in a step may still result in high yield of desired products. Second, Diels–Alder reactions feature prominently in Figures 5 and 7; while synthesis of ethylbenzene from 1,3-butadiene^{84,85} and aromatics from furans and ethylene (Table 1, entry I) have been reported, the reaction of furans with dienes (seen, for instance, in the alternative route to propyl cyclohexane in Figure 5) is novel and expected to be feasible. Third, the formation of acetone from acetic acid in Figure 5 is a well-documented ketonization reaction (Table 1, entry III), although base catalysts can also enable subsequent aldol condensation products. Fourth, pentadiene can be formed via dehydro-decyclization of 2-methyl furan (Table 1, entry IV), as seen in the pathway for propyl cyclohexane in Figure 5; the subsequent Diels–Alder reaction of pentadiene with butadiene has not been reported but is likely feasible, albeit with additional (self) Diels–Alder byproducts.

It should be noted that all 109 candidates require six or more steps (Figure S14 in Section S4). The capital and operating costs increase with every additional reaction due to the need for multiple reactors and separation units. Economical synthesis of SAFs would require process intensification by integrating several steps in a single reactor. For instance, combining metal and acid functionalities in a single reactor (a multifunctional catalyst or a physical mixture of multiple catalysts) could allow cascades of hydrogenation, HDO, and dehydration in a “single” pot and plausibly couple fast exergonic steps with slow endergonic ones.¹⁰⁴ For instance, the last few steps in the pathways shown in Figures 5 and 7 all involve hydrogenation and HDO steps that can be

combined in a single pot. However, this could result in a mixture of products, not all of which are fuel candidates. Our results chart the space of possibilities, identifying the optimal process further requires leveraging this information within a concerted effort in catalyst selection, reaction engineering, and process systems engineering.

CONCLUSIONS

Current pathways to produce SAFs from alcohols and fatty acids lack cycloalkane and aromatic molecules, produce a small fuel volume that cannot meet the growing demand, and exhibit high cost. Alternative pathways are urgently needed. Here, we used an automated network generation based on typical organic chemistry reaction rules to produce a rich reaction network of 223,107 species among 363,840 reactions from furanics (produced from lignocellulose and hemicellulose) and acetic acid, as starting reagents, to demonstrate the approach. Several aromatics and cycloalkanes were found, indicating furanics are excellent platform molecules for making SAFs. In contrast, iso-alkanes have rarely been seen; their production requires exploring other reagents and longer routes. To prune the vast chemical space, first we sought molecules with the right number of carbon numbers (C₈–C₁₆) and high energy density without containing oxygen, as rudimentary fuel properties. Second, we limited the number of reaction steps to reduce cost. Data-driven thermochemistry estimation of the heat of formation then identified >100 alkanes over >300 synthesis routes as potential SAF candidates. Interestingly, many of the molecules we predicted have never been reported before; their pathways, while plausible, as evidenced by reactions reported in the literature, are nonintuitive, thereby underlining the need for our novel approach. Next, we introduced pathway surrogates of energy use (estimated using thermochemistry) and process-chemistry-related CO₂ emissions stemming from the reaction stoichiometry due to carbon loss and H₂ use due to the exothermicity of the methane steam reformer. We found many paths with GWP in the range of 0.7–1 kg-CO₂/kg-product. Promising SAFs and synthesis routes for low net CO₂ emissions may not be the ones producing the highest energy density molecules; a trade-off exists. While we showed pathways to the most energy-dense candidates and those with the lowest CO₂ emissions, these only cover a small subset of the 109 plausible candidates. The interactive tool provided here (see Section S5 for instructions) will enable extracting pathways to the rest of the molecules.

Our network generation and simple fuel properties and GWP metrics indicate a rich chemical space for making SAFs, even though (i) we restricted our search to well-proven chemistries (as rule inputs to RING), (ii) we sought short pathways as a means to minimize capital investment, and (iii) we considered no heat integration as a worst-case scenario. The optimal molecules and synthesis route need to be concurrently designed considering cost and CO₂ footprint of: (1) the biomass-derived reactants, including land use, water, etc., (2) any hydrogen used for upgrading, (3) the energy required for the reactions, (4) the energy required for separations, pumps, etc., (5) the theoretical carbon loss due to the chemistry, and (6) actual reaction yields leading to byproducts. Such a thorough exploration is predicated on the availability of fast methods, semiempirical or artificial intelligence-based, to estimate thermophysical, kinetic, and economic properties. The relatively large number of steps necessitates designing intensified processes integrating multiple

reaction steps into multifunctional catalytic reactors. Experimental demonstrations are also needed.

ASSOCIATED CONTENT

Supporting Information

The Supporting Information is available free of charge at <https://pubs.acs.org/doi/10.1021/acssuschemeng.4c04199>.

Input (.ring) and output files of RING, scripts for specific energy computation (jet_energy folder) and stoichiometry computation (.py), the queried pathways for all SAF molecules (Pathway_109_processed), and an interactive tool for searching SAF molecules and pathways in the extracted results; description of rules, a figure of all 109 SAF molecular candidates, details of pathway fingerprint generation and the correlation analysis between reactants and chemistries, a collection of supplementary figures including: (1) the distribution of species found in the studied reaction network, (2) histogram of reactants employed and histogram of reaction rules employed for the found SAF molecular candidates, (3) the lowest “EndoSum”, “AbsdHsum” and “CO_{2eq}” pathways illustration of the top 3 energy-dense molecules, (4) a histogram and a correlation analysis of hydrogen consumption, water and carbon dioxide generation for the pathways to all SAF molecular candidates, (5) a list of molecules with the lowest and the second lowest CO_{2eq}, (6) the “min-max”, “Endo-Sum” and “AbsdHsum” pathways illustration of the two molecules with lowest and the second lowest CO_{2eq}, (7) a list of molecules with non-100% carbon atom efficiency, (8) a histogram of min number of steps and rank required in producing all found SAF molecular candidates, and (9) a user instruction of the SAF molecules and pathways searching tool ([ZIP](#))

AUTHOR INFORMATION

Corresponding Authors

Srinivas Rangarajan – Department of Chemical and Biomolecular Engineering, Lehigh University, Bethlehem, Pennsylvania 18015, United States;  orcid.org/0000-0002-6777-9421; Email: srr516@lehigh.edu

Dionisios G. Vlachos – Department of Chemical and Biomolecular Engineering, University of Delaware, Newark, Delaware 19711, United States; Catalysis Center for Energy Innovation and Delaware Energy Institute, Newark, Delaware 19716, United States;  orcid.org/0000-0002-6795-8403; Email: vlachos@udel.edu

Authors

Chin-Fei Chang – Department of Chemical and Biomolecular Engineering, Lehigh University, Bethlehem, Pennsylvania 18015, United States

Kristin Paragian – Department of Chemical and Biomolecular Engineering, University of Delaware, Newark, Delaware 19711, United States; Catalysis Center for Energy Innovation and Delaware Energy Institute, Newark, Delaware 19716, United States

Sunitha Sadula – Department of Chemical and Biomolecular Engineering, University of Delaware, Newark, Delaware 19711, United States; Catalysis Center for Energy Innovation and Delaware Energy Institute, Newark, Delaware 19716, United States

Complete contact information is available at: <https://pubs.acs.org/10.1021/acssuschemeng.4c04199>

Author Contributions

C.C. and K.P. contributed equally to this work.

Notes

The authors declare no competing financial interest.

ACKNOWLEDGMENTS

K.P., S.D., and D.G.V. were supported as part of the Catalysis Center for Energy Innovation, an Energy Frontier Research Center funded by the US Dept. of Energy, Office of Science, Office of Basic Energy Sciences under award number DE-SC0001004. S.R. acknowledges support from the National Science Foundation (CBET program) under award numbers 2045550 and 1953245. Portions of this research were conducted on Lehigh University’s Research Computing infrastructure partially supported by NSF Award 2019035. The authors thank T.J. Xie and Eric Chen for performing density functional theory (DFT) calculations to compute the contributions of missing groups to overall enthalpy.

REFERENCES

- (1) *Climate Action Plan*; Federal Aviation Administration: United States, 2021.
- (2) Muratori, M.; Kunz, T.; Hula, A.; Freedberg, M. *US National Blueprint for Transportation Decarbonization: A Joint Strategy to Transform Transportation*; Department of Energy. Office of Energy Efficiency and…: United States, 2023.
- (3) Gössling, S.; Humpe, A.; Fichert, F.; Creutzig, F. COVID-19 and pathways to low-carbon air transport until 2050. *Environ. Res. Lett.* **2021**, *16* (3), No. 034063.
- (4) Sustainable Aviation Fuel Grand Challenge. Energy.gov., 2023. <https://www.energy.gov/eere/bioenergy/sustainable-aviation-fuel-grand-challenge>. Accessed July 2024.
- (5) Davis, M.; Langholtz, M. *Woody Biomass for the Developing Bioeconomy, a Billion-ton Report Update*; EGU General Assembly: Vienna, Austria, 2024.
- (6) Holladay, J.; Abdullah, Z.; Heyne, J. *Sustainable Aviation Fuel: Review of Technical Pathways*; Department of Energy: Washington, DC, USA, 2020.
- (7) Edwards, J. T. In *Reference Jet Fuels for Combustion Testing*, 55th AIAA Aerospace Sciences Meeting; ARC, 2017; p 0146.
- (8) ICAO, 2024. <https://www.icao.int/environmental-protection/GFAAF/Pages/Conversion-processes.aspx>. Accessed July.
- (9) Yang, Z.; Xu, Z.; Feng, M.; Cort, J.; Gieleciak, R.; Heyne, J.; Yang, B. Lignin-based jet fuel and its blending effect with conventional jet fuel. *Fuel* **2022**, *321*, No. 124040.
- (10) Faulhaber, C.; Kosir, S. T.; Borland, C.; Gawełek, K.; Boehm, R. C.; Heyne, J. S. In *Optical Dilatometry Measurements for the Quantification of Sustainable Aviation Fuel Materials Compatibility*, AIAA SCITECH 2022 Forum; ARC, 2022.
- (11) Boehm, R. C.; Yang, Z.; Heyne, J. Threshold Sooting Index of Sustainable Aviation Fuel Candidates from Composition Input Alone: Progress toward Uncertainty Quantification. *Energy Fuels* **2022**, *36*, 1916–1928.
- (12) Kramer, S.; Andac, G.; Heyne, J.; Ellsworth, J.; Herzig, P.; Lewis, K. C. Perspectives on fully synthesized sustainable aviation fuels: direction and opportunities. *Front. Energy Res.* **2022**, *9*, No. 782823.
- (13) Yang, Z.; Bell, D. C.; Boehm, R.; Marques, P. F.; Boze, J. A.; Kosilkina, I. V.; Heyne, J. *Assessing the Effect of Composition on Dielectric Constant of Sustainable Aviation Fuel*; SSRN, 2024.
- (14) Woodroffe, J.-D.; Harvey, B. G. High-performance, biobased, jet fuel blends containing hydrogenated monoterpenes and synthetic paraffinic kerosenes. *Energy Fuels* **2020**, *34* (5), 5929–5937.

- (15) Muldoon, J. A.; Harvey, B. G. Bio-Based Cycloalkanes: The Missing Link to High-Performance Sustainable Jet Fuels. *ChemSusChem* **2020**, *13* (22), 5777–5807.
- (16) Morris, D. M.; Quintana, R. L.; Harvey, B. G. High-performance jet fuels derived from bio-based alkenes by iron-catalyzed [2+ 2] cycloaddition. *ChemSusChem* **2019**, *12* (8), 1646–1652.
- (17) Rosenkoetter, K. E.; Kennedy, C. R.; Chirik, P. J.; Harvey, B. G. [4+ 4]-cycloaddition of isoprene for the production of high-performance bio-based jet fuel. *Green Chem.* **2019**, *21* (20), 5616–5623.
- (18) Li, G.; Hou, B.; Wang, A.; Xin, X.; Cong, Y.; Wang, X.; Li, N.; Zhang, T. Making JP-10 superfuel affordable with a lignocellulosic platform compound. *Angew. Chem., Int. Ed.* **2019**, *58* (35), 12154–12158.
- (19) Deng, Q.; Nie, G.; Pan, L.; Zou, J.-J.; Zhang, X.; Wang, L. Highly selective self-condensation of cyclic ketones using MOF-encapsulating phosphotungstic acid for renewable high-density fuel. *Green Chem.* **2015**, *17* (8), 4473–4481.
- (20) Wang, W.; Li, N.; Li, G.; Li, S.; Wang, W.; Wang, A.; Cong, Y.; Wang, X.; Zhang, T. Synthesis of renewable high-density fuel with cyclopentanone derived from hemicellulose. *ACS Sustainable Chem. Eng.* **2017**, *5* (2), 1812–1817.
- (21) Nie, G.; Zhang, X.; Pan, L.; Han, P.; Xie, J.; Li, Z.; Xie, J.; Zou, J.-J. Hydrogenated intramolecular cyclization of diphenylmethane derivatives for synthesizing high-density biofuel. *Chem. Eng. Sci.* **2017**, *173*, 91–97.
- (22) Beck, T.; Blank, B.; Jones, C.; Woods, E.; Cortright, R. Production of Aromatics from di- and Polyoxygenates. WO Patent WO2014152370A2, 2016.
- (23) Stone, M. L.; Webber, M. S.; Mounfield, W. P.; Bell, D. C.; Christensen, E.; Morais, A. R.; Li, Y.; Anderson, E. M.; Heyne, J. S.; Beckham, G. T.; Román-Leshkov, Y. Continuous hydrodeoxygenation of lignin to jet-range aromatic hydrocarbons. *Joule* **2022**, *6* (10), 2324–2337.
- (24) Peters, M. A.; Alves, C. T.; Onwudili, J. A. A Review of Current and Emerging Production Technologies for Biomass-Derived Sustainable Aviation Fuels. *Energies* **2023**, *16* (16), No. 6100.
- (25) Cheng, J.; Li, T.; Huang, R.; Zhou, J.; Cen, K. Optimizing catalysis conditions to decrease aromatic hydrocarbons and increase alkanes for improving jet biofuel quality. *Bioresour. Technol.* **2014**, *158*, 378–382.
- (26) Wang, M.; He, M.; Fang, Y.; Baeyens, J.; Tan, T. The Ni-Mo/ γ -Al₂O₃ catalyzed hydrodeoxygenation of FAME to aviation fuel. *Catal. Commun.* **2017**, *100*, 237–241.
- (27) Hashmi, S. F.; Meriö-Talvio, H.; Hakonen, K. J.; Ruututunen, K.; Sixta, H. Hydrothermolysis of organosolv lignin for the production of bio-oil rich in monoaromatic phenolic compounds. *Fuel Process. Technol.* **2017**, *168*, 74–83.
- (28) Barbaro, P.; Liguori, F.; Moreno-Marrodan, C. Selective direct conversion of C 5 and C 6 sugars to high added-value chemicals by a bifunctional, single catalytic body. *Green Chem.* **2016**, *18* (10), 2935–2940.
- (29) Wang, T.; Tan, J.; Qiu, S.; Zhang, Q.; Long, J.; Chen, L.; Ma, L.; Li, K.; Liu, Q.; Zhang, Q. Liquid fuel production by aqueous phase catalytic transformation of biomass for aviation. *Energy Procedia* **2014**, *61*, 432–435.
- (30) Hronec, M.; Fulajtárova, K.; Liptaj, T.; Stolcová, M.; Prónayová, N.; Soták, T. Cyclopentanone: A raw material for production of C₁₅ and C₁₇ fuel precursors. *Biomass Bioenergy* **2014**, *63*, 291–299.
- (31) Solhy, A.; Amer, W.; Karkouri, M.; Tahir, R.; El Bouari, A.; Fihri, A.; Bousmina, M.; Zahouily, M. Bi-functional modified-phosphate catalyzed the synthesis of α - α' -(EE)-bis(benzylidene)-cycloalkanones: Microwave versus conventional-heating. *J. Mol. Catal. A: Chem.* **2011**, *336*, 8–15.
- (32) Abaee, M. S.; Mojtabedi, M.; Sharifi, R.; Zahedi, M.; Abbasi, H.; Tabar-Heidar, K. Facile synthesis of bis(aryl methylidene)-cycloalkanones mediated by lithium perchlorate under solvent-free conditions. *J. Iran. Chem. Soc.* **2006**, *3*, 293–296.
- (33) Wang, W.; Ji, X.; Ge, H.; Li, Z.; Tian, G.; Shao, X.; Zhang, Q. Synthesis of C₁₅ and C₁₀ fuel precursors with cyclopentanone and furfural derived from hemicellulose. *RSC Adv.* **2017**, *7*, 16901–16907.
- (34) Weingarten, R.; Tompsett, G.; Conner, W.; Huber, G. Design of solid acid catalysts for aqueous-phase dehydration of carbohydrates: The role of Lewis and Bronsted acid sites. *J. Catal.* **2011**, *279*, 174–182.
- (35) Mauritz, K. A.; Moore, R. State of understanding of Nafion. *Chem. Rev.* **2004**, *104*, 4535–4585.
- (36) Cueto, J.; Faba, L.; Díaz, E.; Ordóñez, S. Enhancement of furfural-cyclopentanone aldol condensation using binary water-ethanol mixtures as solvent. *J. Chem. Technol. Biotechnol.* **2018**, *93*, 1563–1571.
- (37) Cueto, J.; Faba, L.; Díaz, E.; Ordóñez, S. Cyclopentanone as an Alternative Linking Reactant for Heterogeneously Catalyzed Furfural Aldol Condensation. *ChemCatChem* **2017**, *9*, 1765–1770.
- (38) Deng, Q.; Xu, J.; Han, P.; Pan, L.; Wang, L.; Zhang, X.; Zou, J. Efficient synthesis of high-density aviation biofuel via solvent-free aldol condensation of cyclic ketones and furanic aldehydes. *Fuel Process. Technol.* **2016**, *148*, 361–366.
- (39) Pino, N.; Hincapié, G.; López, D. Selective Catalytic Route for the Synthesis of High-Density Biofuel Using Biomass-Derived Compounds. *Energy Fuels* **2018**, *32*, 561–573.
- (40) Mantri, K.; Dejaegere, E.; Baron, G.; Denayer, J. Alkylation of bromobenzene with allyl acetate over zeolites: Influence of zeolite factors and reaction conditions on activity and selectivity. *Appl. Catal., A* **2007**, *318*, 95–107.
- (41) Lup, A. N. K.; Abnisa, F.; Daud, W.; Aroua, M. A review on reaction mechanisms of metal-catalyzed deoxygenation process in bio-oil model compounds. *Appl. Catal., A* **2017**, *541*, 87–106.
- (42) Kumar, C. R.; Rambabu, N.; Lingaiah, N.; Prasad, P.; Dalai, A. Hafnium salts of dodeca-tungstophosphoric acid catalysts for liquid phase benzylation of anisole with dibenzylether. *Appl. Catal., A* **2014**, *471*, 1–11.
- (43) Pálunkó, I.; Török, B.; Prakash, G.; Olah, G. Dehydration-rehydration characteristics of Nafion-H, Nafion-H supported on silica and Nafion-H silica nanocomposite catalysts studied by Infrared Microscopy. *J. Mol. Struct.* **1999**, *482–483*, 29–32.
- (44) Lee, W.-S.; Wang, Z.; Wu, R.; Bhan, A. Selective vapor-phase hydrodeoxygenation of anisole to benzene on molybdenum carbide catalysts. *J. Catal.* **2014**, *319*, 44–53.
- (45) Nie, G.; Zhang, X.; Pan, L.; Han, P.; Xie, J.; Li, Z.; Xie, J.; Zou, J. Hydrogenated intramolecular cyclization of diphenylmethane derivatives for synthesizing high-density biofuel. *Chem. Eng. Sci.* **2017**, *173*, 91–97.
- (46) Jing, Y.; Xia, Q.; Xie, J.; Liu, X.; Guo, Y.; Zou, J.; Wang, Y. Robinson Annulation-Directed Synthesis of Jet-Fuel-Ranged Alkylcyclohexanes from Biomass-Derived Chemicals. *ACS Catal.* **2018**, *8*, 3280–3285.
- (47) Arias-Ugarte, R.; Wekesa, F.; Findlater, M. Selective aldol condensation or cyclotrimerization reactions catalyzed by FeCl₃. *Tetrahedron Lett.* **2015**, *56*, 2406–2411.
- (48) Li, H.; Xu, Z.; Yan, P.; Zhang, Z. A catalytic aldol condensation system enables one pot conversion of biomass saccharides to biofuel intermediates. *Green Chem.* **2017**, *19*, 1751–1756.
- (49) Deng, Q.; Nie, G.; Pan, L.; Zou, J.; Zhang, X.; Wang, L. Highly selective self-condensation of cyclic ketones using MOF-encapsulating phosphotungstic acid for renewable high-density fuel. *Green Chem.* **2015**, *17*, 4473–4481.
- (50) Yang, J.; Li, N.; Li, G.; Wang, W.; Wang, A.; Wang, X.; Cong, Y.; Zhang, T. Synthesis of renewable high-density fuels using cyclopentanone derived from lignocellulose. *Chem. Commun.* **2014**, *50*, 2572–2574.
- (51) He, J.; Zhao, C.; Lercher, J. Ni-Catalyzed Cleavage of Aryl Ethers in the Aqueous Phase. *J. Am. Chem. Soc.* **2012**, *134*, 20768–20775.

- (52) Wang, W.; Li, N.; Li, G.; Li, S.; Wang, W.; Wang, A.; Cong, Y.; Wang, X.; Zhang, T. Synthesis of Renewable High-Density Fuel with Cyclopentanone Derived from Hemicellulose. *ACS Sustainable Chem. Eng.* **2017**, *S*, 1812–1817.
- (53) Sheng, X.; Li, N.; Li, G.; Wang, W.; Yang, J.; Cong, Y.; Wang, A.; Wang, X.; Zhang, T. Synthesis of high density aviation fuel with cyclopentanol derived from lignocellulose. *Sci. Rep.* **2015**, *5*, No. 9565, DOI: 10.1038/srep09565.
- (54) Li, G.; Li, N.; Wang, X.; Sheng, X.; Li, S.; Wang, A.; Cong, Y.; Wang, X.; Zhang, T. Synthesis of Diesel or Jet Fuel Range Cycloalkanes with 2-Methylfuran and Cyclopentanone from Lignocellulose. *Energy Fuels* **2014**, *28*, 5112–5118.
- (55) Deng, Q.; Han, P.; Xu, J.; Zou, J.; Wang, L.; Zhang, X. Highly controllable and selective hydroxyalkylation/alkylation of 2-methylfuran with cyclohexanone for synthesis of high-density biofuel. *Chem. Eng. Sci.* **2015**, *138*, 239–243.
- (56) Zhong, Y.; Zhang, P.; Zhu, X.; Li, H.; Deng, Q.; Wang, J.; Zeng, Z.; Zou, J.; Deng, S. Highly Efficient Alkylation Using Hydrophobic Sulfonic Acid-Functionalized Biochar as a Catalyst for Synthesis of High-Density Biofuels. *ACS Sustainable Chem. Eng.* **2019**, *7*, 14973–14981.
- (57) Huang, S.; Luo, X.; Li, J.; Liu, S.; Shuai, L. Selective production of bicyclic alkanes as high-density fuel additives by coupling lignocellulose-derived furanics and phenolics. *Green Chem.* **2024**, *26*, 4043–4050.
- (58) Li, Z.; Jiang, Y.; Li, Y.; Zhang, H.; Li, H.; Yang, S. Advances in Diels–Alder/aromatization of biomass furan derivatives towards renewable aromatic hydrocarbons. *Catal. Sci. Technol.* **2022**, *12* (6), 1902–1921.
- (59) Wang, D.; Osmundsen, C. M.; Taarning, E.; Dumescic, J. A. Selective production of aromatics from alkylfurans over solid acid catalysts. *ChemCatChem* **2013**, *5* (7), 2044–2050.
- (60) Chang, C.-C.; Green, S. K.; Williams, C. L.; Dauenhauer, P. J.; Fan, W. Ultra-selective cycloaddition of dimethylfuran for renewable p-xylene with H-BEA. *Green Chem.* **2014**, *16* (2), 585–588.
- (61) Zhao, R.; Zhao, Z.; Li, S.; Parvulescu, A. N.; Müller, U.; Zhang, W. Excellent Performances of Dealuminated H-Beta Zeolites from Organotemplate-Free Synthesis in Conversion of Biomass-derived 2, 5-Dimethylfuran to Renewable p-Xylene. *ChemSusChem* **2018**, *11* (21), 3803–3811.
- (62) Cho, H. J.; Ren, L.; Vattipalli, V.; Yeh, Y. H.; Gould, N.; Xu, B.; Gorte, R. J.; Lobo, R.; Dauenhauer, P. J.; Tsapatsis, M.; Fan, W. Renewable p-Xylene from 2, 5-Dimethylfuran and Ethylene Using Phosphorus-Containing Zeolite Catalysts. *ChemCatChem* **2017**, *9* (3), 398–402.
- (63) Williams, C. L.; Chang, C.-C.; Do, P.; Nikbin, N.; Caratzoulas, S.; Vlachos, D. G.; Lobo, R. F.; Fan, W.; Dauenhauer, P. J. Cycloaddition of biomass-derived furans for catalytic production of renewable p-xylene. *ACS Catal.* **2012**, *2* (6), 935–939.
- (64) Corma, A.; de la Torre, O.; Renz, M.; Villandier, N. Production of high-quality diesel from biomass waste products. *Angew. Chem., Int. Ed.* **2011**, *50* (10), 2375–2378.
- (65) Li, S.; Li, N.; Li, G.; Li, L.; Wang, A.; Cong, Y.; Wang, X.; Zhang, T. Lignosulfonate-based acidic resin for the synthesis of renewable diesel and jet fuel range alkanes with 2-methylfuran and furfural. *Green Chem.* **2015**, *17* (6), 3644–3652.
- (66) Liu, S.; Dutta, S.; Zheng, W.; Gould, N. S.; Cheng, Z.; Xu, B.; Saha, B.; Vlachos, D. G. Catalytic hydrodeoxygenation of high carbon furylmethanes to renewable jet-fuel ranged alkanes over a rhenium-modified iridium catalyst. *ChemSusChem* **2017**, *10* (16), 3225–3234.
- (67) Dutta, S.; Bohre, A.; Zheng, W.; Jenness, G. R.; Núñez, M.; Saha, B.; Vlachos, D. G. Solventless C–C coupling of low carbon furanics to high carbon fuel precursors using an improved graphene oxide carbocatalyst. *ACS Catal.* **2017**, *7* (6), 3905–3915.
- (68) Bohre, A.; Dutta, S.; Saha, B.; Abu-Omar, M. M. Upgrading furfurals to drop-in biofuels: An overview. *ACS Sustainable Chem. Eng.* **2015**, *3* (7), 1263–1277.
- (69) Liu, S.; Josephson, T. R.; Athaley, A.; Chen, Q. P.; Norton, A.; Ierapetritou, M.; Siepmann, J. I.; Saha, B.; Vlachos, D. G. Renewable lubricants with tailored molecular architecture. *Sci. Adv.* **2019**, *5* (2), No. eaav5487.
- (70) Goculdas, T.; Korathotage, K.; Montone, C.; Sadula, S.; Bloch, E. D.; Vlachos, D. G. Synthesis of Long Chain Oxygenates via Aldol Condensation of Furfural and Acetone over Metal–Organic Frameworks. *ACS Appl. Mater. Interfaces* **2023**, *15* (49), 57070–57078.
- (71) Goculdas, T.; Deshpande, S.; Zheng, W.; Gorte, R. J.; Sadula, S.; Vlachos, D. G. Highly selective cross ketonization of renewable acids over magnesium oxide. *Green Chem.* **2023**, *25* (2), 614–626.
- (72) Park, D. S.; Joseph, K. E.; Koehle, M.; Krumm, C.; Ren, L.; Damen, J. N.; Shete, M. H.; Lee, H. S.; Zuo, X.; Lee, B.; et al. Tunable oleo-furan surfactants by acylation of renewable furans. *ACS Cent. Sci.* **2016**, *2* (11), 820–824.
- (73) Nguyen, H.; Wang, Y.; Moglia, D.; Fu, J.; Zheng, W.; Orazov, M.; Vlachos, D. G. Production of renewable oleo-furan surfactants by cross-ketonization of biomass-derived furoic acid and fatty acids. *Catal. Sci. Technol.* **2021**, *11* (8), 2762–2769.
- (74) Rangarajan, S.; Bhan, A.; Daoutidis, P. Language-oriented rule-based reaction network generation and analysis: Description of RING. *Comput. Chem. Eng.* **2012**, *45*, 114–123.
- (75) Rangarajan, S.; Bhan, A.; Daoutidis, P. Rule-Based Generation of Thermochemical Routes to Biomass Conversion. *Ind. Eng. Chem. Res.* **2010**, *49* (21), 10459–10470.
- (76) Panagiotopoulou, P.; Vlachos, D. G. Liquid phase catalytic transfer hydrogenation of furfural over a Ru/C catalyst. *Appl. Catal., A* **2014**, *480*, 17–24.
- (77) Gilkey, M. J.; Panagiotopoulou, P.; Mironenko, A.; Jenness, G.; Vlachos, D.; Xu, B. Mechanistic Insights into Metal Lewis Acid-Mediated Catalytic Transfer Hydrogenation of Furfural to 2-Methylfuran. *ACS Catal.* **2015**, *5*, 3988–3994.
- (78) Hsiao, Y. W.; Zong, X.; Zhou, J.; Zheng, W.; Vlachos, D. Selective hydrodeoxygenation of 5-hydroxymethylfurfural (HMF) to 2,5-dimethylfuran (DMF) over carbon supported copper catalysts using isopropyl alcohol as a hydrogen donor. *Appl. Catal., B* **2022**, *317*, No. 121790.
- (79) Cohen, N.; Benson, S. W. Estimation of Heats of Formation of Organic-Compounds by Additivity Methods. *Chem. Rev.* **1993**, *93* (7), 2419–2438.
- (80) Wittreich, G. R.; Vlachos, D. G. Python Group Additivity (pGrAdd) software for estimating species thermochemical properties. *Comput. Phys. Commun.* **2022**, *273*, No. 108277.
- (81) Lange, J.-P. Fuels and Chemicals Manufacturing; Guidelines for Understanding and Minimizing the Production Costs. *Cattech* **2001**, *5* (2), 82–95.
- (82) EPA Technical Support Document for Hydrogen Production: Proposed Rule for Mandatory Reporting of Greenhouse Gases, 2024. https://www.epa.gov/sites/default/files/2015-02/documents/subpartp-tsd_hydrogenproduction.pdf. Accessed July.
- (83) Li, G. Y.; Li, N.; Yang, J. F.; Wang, A. Q.; Wang, X. D.; Cong, Y.; Zhang, T. Synthesis of renewable diesel with the 2-methylfuran, butanal and acetone derived from lignocellulose. *Bioresour. Technol.* **2013**, *134*, 66–72.
- (84) Chang, J. S.; Park, S. E.; Gao, Q. M.; Férey, G.; Cheetham, A. K. Catalytic conversion of butadiene to ethylbenzene over the nanoporous nickel(II) phosphate, VSB-1. *Chem. Commun.* **2001**, No. 9, 859–860.
- (85) Settle, A. E.; Berstis, L.; Rorrer, N. A.; Roman-Leshkov, Y.; Beckham, G. T.; Richards, R. M.; Vardon, D. R. Heterogeneous Diels–Alder catalysis for biomass-derived aromatic compounds. *Green Chem.* **2017**, *19* (15), 3468–3492.
- (86) Williams, C. L.; Chang, C. C.; Do, P.; Nikbin, N.; Caratzoulas, S.; Vlachos, D. G.; Lobo, R. F.; Fan, W.; Dauenhauer, P. J. Cycloaddition of Biomass-Derived Furans for Catalytic Production of Renewable p-Xylene. *ACS Catal.* **2012**, *2* (6), 935–939.
- (87) Nikbin, N.; Do, P. T.; Caratzoulas, S.; Lobo, R. F.; Dauenhauer, P. J.; Vlachos, D. G. A DFT study of the acid-catalysed conversion of 2,5-dimethylfuran and ethylene to p-xylene. *J. Catal.* **2013**, *297*, 35–43.

- (88) Patet, R. E.; Nikbin, N.; Williams, C. L.; Green, S. K.; Chang, C.-C.; Fan, W.; Caratzoulas, S.; Dauenhauer, P. J.; Vlachos, D. G. Kinetic Regime Change in the Tandem Dehydrative Aromatization of Furan Diels–Alder Products. *ACS Catal.* **2015**, *5* (4), 2367–2375.
- (89) Green, S. K.; Patet, R. E.; Nikbin, N.; Williams, C. L.; Chang, C. C.; Yu, J. Y.; Gorte, R. J.; Caratzoulas, S.; Fan, W.; Vlachos, D. G.; Dauenhauer, P. J. Diels-Alder cycloaddition of 2-methylfuran and ethylene for renewable toluene. *Appl. Catal., B* **2016**, *180*, 487–496.
- (90) Williams, C. L.; Vinter, K. P.; Chang, C. C.; Xiong, R. C.; Green, S. K.; Sandler, S. I.; Vlachos, D. G.; Fan, W.; Dauenhauer, P. J. Kinetic regimes in the tandem reactions of H-BEA catalyzed formation of p-xylene from dimethylfuran. *Catal. Sci. Technol.* **2016**, *6* (1), 178–187.
- (91) Nguyen, H.; Wang, Y. Z.; Moglia, D.; Fu, J. Y.; Zheng, W. Q.; Orazov, M.; Vlachos, D. G. Production of renewable oleo-furan surfactants by cross-ketonization of biomass-derived furoic acid and fatty acids. *Catal. Sci. Technol.* **2021**, *11* (8), 2762–2769.
- (92) Liu, S. B.; Dutta, S.; Zheng, W. Q.; Gould, N. S.; Cheng, Z. W.; Xu, B. J.; Saha, B.; Vlachos, D. G. Catalytic Hydrodeoxygenation of High Carbon Furylmethanes to Renewable Jet-fuel Ranged Alkanes over a Rhodium-Modified Iridium Catalyst. *ChemSusChem* **2017**, *10* (16), 3225–3234.
- (93) Liu, S. B.; Josephson, T. R.; Athaley, A.; Chen, Q. P.; Norton, A.; Ierapetritou, M.; Siepmann, J. I.; Saha, B.; Vlachos, D. G. Renewable lubricants with tailored molecular architecture. *Sci. Adv.* **2019**, *5* (2), No. eaav5487.
- (94) Liu, S. B.; Saha, B.; Vlachos, D. G. Catalytic production of renewable lubricant base oils from bio-based 2-alkylfurans and enals. *Green Chem.* **2019**, *21* (13), 3606–3614.
- (95) Saha, B.; Vlachos, D. G. Bio-based lubricant base-oils: Tuning synthesis to meet market desirability. *Catal. Rev.* **2019**, *32* (5), 1–6.
- (96) Liu, S. B.; Bhattacharjee, R.; Li, S.; Danielson, A.; Mazal, T.; Saha, B.; Vlachos, D. G. Thiol-promoted catalytic synthesis of high-performance furan-containing lubricant base oils from biomass derived 2-alkylfurans and ketones. *Green Chem.* **2020**, *22* (22), 7896–7906.
- (97) Saha, B.; Vlachos, D. G. Synthesis of (hemi)cellulosic lubricant base oils via catalytic coupling and deoxygenation pathways. *Green Chem.* **2021**, *23* (14), 4916–4930.
- (98) Abdelrahman, O. A.; Park, D. S.; Vinter, K. P.; Spanjers, C. S.; Ren, L.; Cho, H. J.; Vlachos, D. G.; Fan, W.; Tsapatsis, M.; Dauenhauer, P. J. Biomass-Derived Butadiene by Dehydra-Decyclization of Tetrahydrofuran. *ACS Sustainable Chem. Eng.* **2017**, *5* (5), 3732–3736.
- (99) Li, S.; Abdelrahman, O. A.; Kumar, G.; Tsapatsis, M.; Vlachos, D. G.; Caratzoulas, S.; Dauenhauer, P. J. Dehydra-Decyclization of Tetrahydrofuran on H-ZSMS: Mechanisms, Pathways, and Transition State Entropy. *ACS Catal.* **2019**, *9* (11), 10279–10293.
- (100) de Mello, M. D.; Kumar, G.; Tabassum, T.; Jain, S. K.; Chen, T. H.; Caratzoulas, S.; Li, X. Y.; Vlachos, D. G.; Han, S. I.; Scott, S. L.; et al. Phosphonate-Modified UiO-66 Bronsted Acid Catalyst and Its Use in Dehydra-Decyclization of 2-Methyltetrahydrofuran to Pentadienes. *Angew. Chem., Int. Ed.* **2020**, *59* (32), 13260–13266.
- (101) Ji, Y. C.; Batchu, S. P.; Lawal, A.; Vlachos, D. G.; Gorte, R. J.; Caratzoulas, S.; Abdelrahman, O. A. Selective dehydra-decyclization of cyclic ethers to conjugated dienes over zirconia. *J. Catal.* **2022**, *410*, 10–21.
- (102) Batchu, S. P.; Caratzoulas, S.; Vlachos, D. G. How Topological Differences between Two Oxide Surfaces Determine Selectivity-The Case of the Dehydra-Decyclization of Tetrahydrofuran. *Chemistry* **2023**, *5* (1), 422–437.
- (103) Ji, Y.; Batchu, S. P.; Lawal, A.; Vlachos, D. G.; Gorte, R. J.; Caratzoulas, S.; Abdelrahman, O. A. Selective dehydra-decyclization of cyclic ethers to conjugated dienes over zirconia. *J. Catal.* **2022**, *410*, 10–21.
- (104) Simonetti, D. A.; Dumesic, J. A. Catalytic Production of Liquid Fuels from Biomass-Derived Oxygenated Hydrocarbons: Catalytic Coupling at Multiple Length Scales. *Catal. Rev.* **2009**, *51* (3), 441–484.